

## Article

# Identification and Transcriptional Profiling of SNARE Family in *Monascus ruber* M7 Reveal Likely Roles in Secondary Metabolism

Chenchen Meng<sup>1</sup>, Youxiang Zhou<sup>2</sup>, Jiao Liu<sup>2,\*</sup> and Fusheng Chen<sup>1,\*</sup> 

<sup>1</sup> Hubei International Scientific and Technological Cooperation Base of Traditional Fermented Foods, College of Food Science and Technology, Huazhong Agricultural University, Wuhan 430070, China

<sup>2</sup> Hubei Key Laboratory of Nutritional Quality and Safety of Agro Products, Institute of Quality Standard and Testing Technology for Agro-Products, Hubei Academy of Agricultural Sciences, Wuhan 430064, China

\* Correspondence: babojiao@126.com (J.L.); chenfs@mail.hzau.edu.cn (F.C.)

**Abstract:** Soluble N-ethylmaleimide-sensitive factor attachment protein receptors (SNAREs) are the core components that mediate vesicle fusion, and they play an important role in secondary metabolism of filamentous fungi. However, in *Monascus* spp., one of the traditional medicinal and edible filamentous fungi, the members and function of SNAREs remain unknown. Here, twenty SNAREs in *M. ruber* M7 were systematically identified based on the gene structure, amino acid structure and phylogenetic analysis and were classified into four subfamilies. We also compared the expression profiles of twenty *MrSNAREs* in *M. ruber* M7 and its deletion mutants,  $\Delta$ *mrpigA* and  $\Delta$ *pksCT*, which could not produce *Monascus* pigment and citrinin, respectively. The results indicated that these *MrSNAREs* showed distinct expression patterns in the three strains. Compared to *M. ruber* M7, the expression levels of *Mrtlg2*, *Mrbet1*, *Mrgos1* and *Mrsec22* remained higher in  $\Delta$ *mrpigA* but lower in  $\Delta$ *pksCT*, which could be reason to consider them as potential candidate genes involved in secondary metabolism for further functional characterization. Further, the significant upregulation of *Mrpep12* and *Mrvtil* in  $\Delta$ *pksCT* is worthy of attention for further research. Our results provide systematic identification and expression profiling of the SNARE family in *Monascus* and imply that the functions of *MrSNAREs* are specific to different secondary metabolic processes.

**Keywords:** SNARE; *Monascus*; expression profile; secondary metabolism



**Citation:** Meng, C.; Zhou, Y.; Liu, J.; Chen, F. Identification and Transcriptional Profiling of SNARE Family in *Monascus ruber* M7 Reveal Likely Roles in Secondary Metabolism. *Fermentation* **2022**, *8*, 750. <https://doi.org/10.3390/fermentation8120750>

Academic Editor: Francesca Berini

Received: 28 November 2022

Accepted: 13 December 2022

Published: 16 December 2022

**Publisher's Note:** MDPI stays neutral with regard to jurisdictional claims in published maps and institutional affiliations.



**Copyright:** © 2022 by the authors. Licensee MDPI, Basel, Switzerland. This article is an open access article distributed under the terms and conditions of the Creative Commons Attribution (CC BY) license (<https://creativecommons.org/licenses/by/4.0/>).

## 1. Introduction

Vesicle transport is the basic form involved in the transportation of substances between different cellular compartments in eukaryotic cells [1–3]. Usually, this cargo includes protein, lipids and secondary metabolites that are carried out by membranous vesicles; then, unique sets of proteins are recruited to finish the subsequent essential steps, including trafficking, binding, fusion and/or retrieval [4,5]. Among them, correct membrane fusion between the vesicle and target membrane is very important to maintain homeostasis, promote growth and regulate secondary metabolism; this relies on the catalysis and regulation of SNAREs (soluble N-ethylmaleimide-sensitive factor attachment protein receptors) [6,7].

Generally, SNARE proteins are widely present in the membranous organelles of eukaryotes, such as the endoplasmic reticulum, Golgi membranes and vacuoles, as well as in the vesicles produced by these organelles [8,9]. Based on the amino acid sequence characteristics of SNARE motifs, SNAREs are classified as Q-SNAREs (syntaxin, SNAP-25) or R-SNAREs (synaptobrevin), which contain highly conserved glutamine (Q) residues and arginine (R) residues, respectively [10]. The Q-SNARE family can be further classified as Qa-, Qb- or Qc-SNAREs based on the amino acid sequence homologies [11]. Alternatively, depending on the location, SNAREs can be divided as v-SNAREs, which are located in vesicles, or t-SNAREs, which are located in target membranes. Moreover, v-SNAREs

usually correspond to R-SNAREs, and t-SNAREs to Q-SNAREs [12]. During vesicle fusion, three Q-SNAREs interact with one R-SNARE to form an extremely stable four-helix bundle, called a SNARE complex or SNAREpin [8,13]. The SNAREpin brings together the vesicle and the target membrane, thereby facilitating their fusion and release of the vesicle's contents [14].

Since the first SNARE was identified in 1993 [15], a variety of SNARE protein-coding genes have been identified in different organisms based on genome-wide identification, such as 36 SNAREs in *Homo sapiens*, 68 SNAREs in *Arabidopsis thaliana* and 24 SNAREs in *Saccharomyces cerevisiae* [13,16,17]. In filamentous fungi, SNAREs exhibit an important regulatory role in their metabolic activities [18]. For example, deletion of *Cfoam7* (vacuole membrane-located Qc-SNARE gene) in *Colletotrichum fructicola* results in defects in vegetative growth, conidiation, appressorium formation and cell wall integrity [19]. Further, some SNAREs are responsible for physiological processes, stress resistance and pathogenicity [20]. The deletion of *FoSyn1* (Qa-SNARE) leads to a decrease in the tolerance of *Falciophora oryzae* to cadmium [21]. Most notably, diverse reports propose that SNAREs also show a major role in fungal secondary metabolism [22,23]. In *Fusarium graminearum*, deletion of Qc-SNARE(*FgSyn8*) significantly reduces the production of deoxynivalenol, and deletion of *MoSyn8* in *Magnaporthe oryzae* reduces melanin pigmentation [18,24].

*Monascus* spp. are famous edible and medicinal filamentous fungi widely applied in Southeast Asian countries for nearly 2000 years [25]. Their rice-based fermentation product, *Hongqu*, is a highly accepted fermentation starter, natural food colorant and folk medicine; it can produce abundant beneficial secondary metabolites, such as *Monascus* pigments (MPs), monacolin K and  $\gamma$ -aminobutyric acid [26,27]. However, some *Monascus* strains can produce citrinin (CIT), a nephrotoxic mycotoxin contaminant in *Hongqu* and related products [28,29]. Therefore, reducing or eliminating the CIT yield and increasing MPs production by *Monascus* is the core problem of industrial mass production. In addition to fermentation condition optimization and strain breeding [30,31], clarifying the understanding of the vesicle transport mechanism of *Monascus* may provide a new idea, but the function of the SNARE family in *Monascus* is still unclear. On this basis, a comprehensive genome-wide analysis of SNARE genes in *M. ruber* M7 (*MrSNAREs*) was performed in this study to explore their potential roles in secondary metabolism. Firstly, the characterizations, gene structures and classifications of all the identified *MrSNAREs* were compared. Then, the *MrSNARE* expression profiles of three *Monascus* strains were analyzed and compared by real-time quantitative PCR (RT-qPCR), which included *M. ruber* M7 (wildtype, producing MPs and CIT),  $\Delta$ *mrpigA* (MPs biosynthetic gene deletion mutant, producing CIT but MPs-free) [32,33] and  $\Delta$ *pksCT* (CIT biosynthetic gene deletion mutant, producing MPs but CIT-free) [34,35]. Finally, the differentially expressed *MrSNAREs* that might be linked to MPs and CIT synthesis were preliminarily discussed. Collectively, this study could provide a data basis for future studies involved in vesicle-transport-system-regulated secondary metabolism in filamentous fungi.

## 2. Materials and Methods

### 2.1. Microbial Strains and Culture Conditions

The wildtype strain *Monascus ruber* M7 was stored in our laboratory; it can produce MPs and CIT simultaneously. The MPs and CIT biosynthetic gene clusters have been analyzed in previous study; based on the results, two mutants,  $\Delta$ *mrpigA* and  $\Delta$ *pksCT*, were constructed by our research group. In detail,  $\Delta$ *mrpigA* is an MPs-free mutant strain in which the MPs polyketide synthases gene (*mrpigA*) has been partly disrupted [33],  $\Delta$ *pksCT* is a CIT-free mutant strain in which the CIT polyketide synthases gene (*pksCT*) has been partly disrupted [35]. These three strains were cultured in potato dextrose agar (PDA) slant medium at 28 °C.

## 2.2. Genome-Wide Identification of SNARE Genes in *Monascus ruber* M7

The amino acid sequences of SNARE genes from *Aspergillus nidulans* and *Saccharomyces cerevisiae* were obtained from the SNARE database (Snare-WebInterface snareMainPage (mpg.de), accessed on 17 December 2020) to identify the homologous SNARE genes in the *M. ruber* M7 genome (Index of /blast/executables/blast+/LATEST (nih.gov), accessed on 30 December 2020). In order to verify the quantity of SNARE homolog genes in *M. ruber* M7 (*MrSNAREs*), the amino acid sequences of candidate *MrSNAREs* were obtained by SoftBerry's FGENESH program (<http://linux1.softberry.com/berry.phtml?topic=fgenes&group=programs&subgroup=gfind>, accessed on 3 January 2021) and then retrieved by NCBI's BLAST program (<https://blast.ncbi.nlm.nih.gov>, accessed on 18 May 2021).

## 2.3. Characterization and Phylogenetic Analysis of Identified *MrSNAREs*

The gene structures of all identified *MrSNAREs* were analyzed by SoftBerry's FGENESH program (<http://linux1.softberry.com/berry.phtml?topic=fgenes&group=programs&subgroup=gfind>, accessed on 3 January 2021), and their visualizations were performed by the Gene Structure Display Server (<http://gsds.gao-lab.org/>, accessed on 15 June 2021). The compute pI/MW tool in the ExpASY database ([http://web.expasy.org/compute\\_pi/](http://web.expasy.org/compute_pi/), accessed on 18 May 2021) was used to calculate the biochemical parameters of *MrSNAREs*. The conserved domains such as the SNARE motif and transmembrane domain (TM) of *MrSNAREs* were annotated by NCBI's CDD program (<http://www.ncbi.nlm.nih.gov/Structure/cdd/wrpsb.cgi>, accessed on 18 May 2021) and the SMART database (SMART: Main page (embl-heidelberg.de), accessed on 18 May 2021). Then, the schematic diagram was prepared by IBS (IBS—Database Visualization (<http://ibs.biocuckoo.org/dbvisualization.php#>, accessed on 29 September 2021)). The properties of the SNARE motif were aligned by MEGA7 software and were adjusted through GeneDoc. Based on this alignment, a phylogenetic tree was constructed with the neighbor-joining method and 1000 bootstrap replications.

## 2.4. MPs and CIT Production Analysis

*M. ruber* M7,  $\Delta pksCT$  and  $\Delta mrpigA$  were inoculated in PDA slant medium and cultured at 28 °C for 12 days. First, the three strains were inoculated on PDA plate medium at 28 °C for 7 d to observe phenotypic characterization. Then, the conidia of *M. ruber* M7,  $\Delta pksCT$  and  $\Delta mrpigA$  were washed with sterile water and collected in a sterile centrifuge tube. After that, 200  $\mu$ L of conidia suspension at a concentration of  $10^5$  cfu/mL was inoculated onto a PDA plate containing cellophane at 28 °C for 11 days. Three replicates were taken for each test sample.

The mycelium and medium were sampled on the 3rd, 7th and 11th days and were dried at 45 °C to measure MPs and CIT production. In detail, dried sample powder (0.1 g) was mixed with 80% methanol solution (4 mL) and ultrasonicated for 30 min. Then, the suspension was centrifuged at 5000 rpm for 10 min; the supernatant was collected and filtered through a 0.22  $\mu$ m nylon filter membrane. Total MPs production was detected by UV spectrophotometer (HITACHI U-3900, Hitachi, Ltd., Chiyoda-ku, Tokyo, Japan) based on the reference method with minor modification [36,37]. The extracts were diluted to an appropriate multiple, and absorbance values were measured at 380, 470 and 520 nm, which are the maximal absorption wavelengths of yellow (YP), orange (OP) and red (RP) pigments, respectively. MPs production was expressed in units of absorbance (U/g). CIT production analysis was performed on a Waters ACQUITYH UPLC I-CLASS system (Waters, Milford, MA, USA). The analytical column was an ACQUITY UPLC BEH C18 (2.1 mm  $\times$  100 mm, 1.7  $\mu$ m; Waters, Milford, MA, USA) maintained at 40 °C. Chromatographic separation was achieved with gradient elution using a complex gradient: mobile phase A was 0.1% formic acid in water, and mobile phase B was acetonitrile. The UPLC gradient program was as follows: 10% B  $\rightarrow$  70% B at 0.01–10.00 min; 70% B  $\rightarrow$  90% B at 10.01–12.00 min; 90% B  $\rightarrow$  10% B at 12.01–15.00 min. The flow rate was 0.3 mL/min with a sample injection volume of 2.0  $\mu$ L.

### 2.5. Gene Expression Analysis by Real-Time Quantitative PCR

The mycelium of *M. ruber* M7,  $\Delta$ *pksCT* and  $\Delta$ *mrpigA* incubated on PDA medium were collected for total RNA extraction on the 3rd and 7th days by using a TransZol Up Plus RNA Kit (TransGen Biotech, Beijing, China). Three biological replicates were taken for each test sample. RNA integrity was visualized by 0.8% agarose gel electrophoresis. RNA concentration and purity ( $OD_{260}/OD_{280}$  ratio > 1.95) were determined with a NanoVolume N-60 Spectroscope (Implen, Munich, Germany). For each sample, the total RNA was reverse transcribed to complementary cDNA using a HiScript<sup>®</sup> II 1st Strand cDNA Synthesis Kit (+gDNA wiper) (Vazyme, R212-02, Nanjing, China). The real-time quantitative PCR (RT-qPCR) reaction was performed by an AceQ<sup>®</sup> qPCR SYBR Green Master Mix (Vazyme, Q111-02, Nanjing, China) following the manufacturer's instructions. The RT-qPCR program was performed as follows: 95 °C for 10 min, followed by 40 cycles at 95 °C for 10 s and 60 °C for 30 s. Automated thermal cycling and data acquisition were performed on a Qtower2.2 system (Analytik Jena AG, Jena, Germany) and qPCRsoft1.1 software. The  $\beta$ -*actin* gene was taken as an internal reference, and the primers used in these analyses are listed in Table S1. The  $2^{-\Delta\Delta C_t}$  method was applied to calculate the fold change of gene transcript levels.

### 2.6. Statistical Analysis

Results are expressed as mean  $\pm$  standard deviation (SD). SPSS 25.0 (Armonk, NY, USA) was utilized for analysis of variance (ANOVA). A heatmap was generated by MetaboAnalyst version 5.0 (<https://www.metaboanalyst.ca>, accessed on 24 August 2022).

## 3. Results

### 3.1. *Monascus ruber* M7 Has 20 SNARE-Encoding Genes

There were 20 putative SNARE genes identified in the *M. ruber* M7 genome, and all of the putative genes were named according to the closest ortholog of *A. nidulans* and *S. cerevisiae* (Table 1). Generally, the identity of SNARE genes between *M. ruber* M7 and *A. nidulans* (29–88%) was higher than that with *S. cerevisiae* (22–67%). The results of gene structure analysis indicated that the putative MrSNAREs possessed 1 to 4 exons, of which, *Mrsyn8* had one exon, *Mrpep12*, *Mrvam7*, *Mrsec9* and *Mrnyv1* had two exons, nine genes (*Mrbet1*, *Mrgos1*, *Mrsec20*, *Mrsnc1*, *Mrtlg1*, *Mrtlg2*, *Mrufe1*, *Mruse1* and *Mrvti1*) had three exons, *Mrsec22*, *Mrsed5* and *Mrssol* had four exons, *Mrykt6* had five exons, and *Mrbos1* and *Mrtom* had seven exons (Figure 1). Sequence analysis showed that the size of the encoded SNARE proteins ranged from 97 to 998 amino acids (aa) (Table 1). Further, their isoelectric points (pIs) ranged from 4.46 (*Mrtlg1*) to 9.83 (*Mrbos1*), and their molecular weights (MWs) ranged from 10,397.74 Da (*Mrbet1*) to 107,978.53 Da (*Mrtom*).

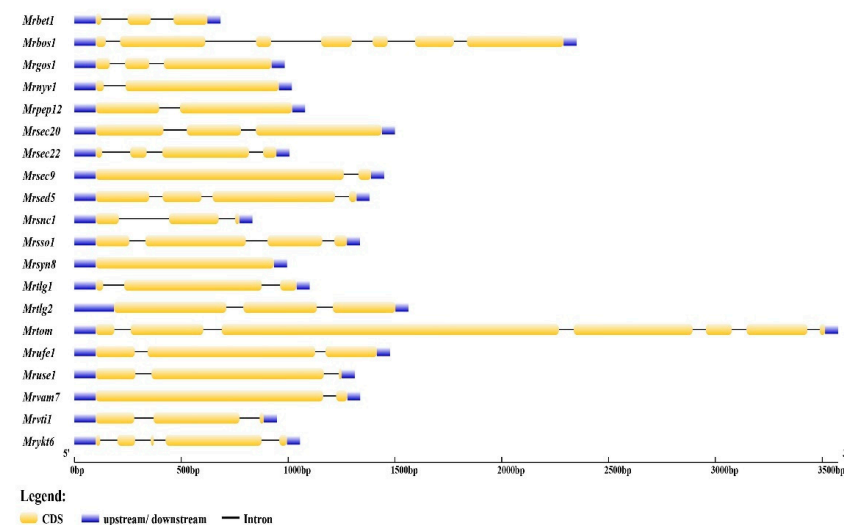


**Figure 1.** Exon–intron structure of MrSNAREs. Blue boxes represent upstream and downstream untranslated regions; yellow boxes represent the CDS; and black lines represent the introns.

**Table 1.** Physicochemical parameters of identified *MrSNAREs*.

Gene Name	GenBank	Length of CDS (bp)	Protein Length (aa)	Molecular Weight (Da)	Isoelectric Point	<i>A. nidulans</i> Identity	<i>S. cerevisiae</i> Identity
<i>Mrpep12</i>	OP620680.1	822	273	30,719.09	5.02	Pep12 (76%)	Pep12 (29%)
<i>Mrssso1</i>	OP620682.1	942	313	34,792.64	5.18	Sso (39%)	Sso1 (25%)
<i>Mrtlg2</i>	OP620686.1	1041	346	45,169.38	6.75	Tlg2 (78%)	Tlg2 (33%)
<i>Mrsed5</i>	OP620683.1	1164	387	38,021.88	9.04	Sed5 (88%)	Sed5 (37%)
<i>Mrufe1</i>	OP620691.1	1209	402	44,159.32	7.21	Ufe1 (49%)	Ufe1 (34%)
<i>Mrbos1</i>	OP620676.1	1365	454	51,257.33	9.83	-	Bos1 (29%)
<i>Mrsec20</i>	OP620689.1	1161	386	43,724.39	5.52	Sec20 (58%)	Sec20 (26%)
<i>Mroti1</i>	OP620690.1	603	200	22,885.51	5.63	Vti1 (79%)	Vti1 (41%)
<i>Mrgos1</i>	OP620693.1	684	227	25,819.33	9.75	Gos1 (86%)	Gos1 (35%)
<i>Mrbet1</i>	OP620679.1	294	97	10,397.74	5.16	Bet1 (29%)	Bet1 (22%)
<i>Mrvam7</i>	OP620681.1	1116	371	41,239.48	9.42	Vam7 (66%)	Vam7 (26%)
<i>Mrtlg1</i>	OP620685.1	756	251	27,983.68	4.46	Tlg1 (70%)	Tlg1 (41%)
<i>Mrsyn8</i>	OP620684.1	834	277	30,575.95	5.04	Syn8 (65%)	Syn8 (24%)
<i>Mruse1</i>	OP620687.1	1080	359	40,026.02	5.14	Use1 (58%)	-
<i>Mrsec9</i>	OP620692.1	1221	406	44,644.99	6.71	Sec9 (63%)	Sec9 (40%)
<i>Mrykt6</i>	OP620694.1	603	200	22,882.07	6.83	Ykt6 (57%)	Ykt6 (53%)
<i>Mrsncl</i>	OP620677.1	360	119	13,012.98	9.39	Snc (71%)	Snc1 (59%)
<i>Mrsec22</i>	OP620678.1	576	171	23,645.99	8.35	Sec22 (79%)	Sec22 (49%)
<i>Mrnyv1</i>	OP620695.1	756	223	27,838.05	9.21	Nyv1 (82%)	Nyv1 (39%)
<i>Mrtom</i>	OP620688.1	2994	988	107,978.53	6.98	Tomosyn (67%)	Sro7 (30%)

### 3.2. Classification of SNARE Genes in *Monascus ruber* M7

The conserved domains of MrSNAREs were analyzed, and the results showed that the MrSNAREs were mainly classified as Qa-, Qb-, Qc- and R-SNAREs (Figure 2). In detail, Qa-SNAREs were composed of five members (*MrSso1p*, *MrPep12p*, *MrSed5p*, *Mrtlg2p* and *MrUfe1p*), which belonged to syntaxin proteins; Qb-SNAREs were composed of five members (*MrBos1p*, *MrGos1p*, *MrVti1p*, *MrSec20p* and *MrSec9N*), which belonged to SNAP-25 N-terminal motif homologous proteins; Qc-SNAREs were composed of five members (*MrBet1p*, *MrSyn8p*, *Mrtlg1p*, *MrUse1p* and *MrSec9C*), which belonged to SNAP-25 C-terminal motif homologous proteins; and R-SNAREs were composed of five members (*MrSnc1p*, *MrSec22p*, *MrNyv1p*, *MrYkt6p* and *MrTomp*), which belonged to synaptobrevin proteins (Figure 2). Ordinarily, the glutamine residues were highly conserved among most Qa-SNAREs, and the arginine residues were highly conserved among all R-SNAREs (Figure 3), while the glutamine residues of one Qb-SNARE (*MrSec20p*) and two Qc-SNAREs (*MrSyn8p* and *MrUse1p*) were replaced by serine (S), histidine (H) or glutamic acid (E) (Figure 3). In addition, phylogenetic analysis indicated that the SNAREs displayed the same four categories described previously (Figure 4). Consistent with the results of multiple sequence alignment, this verifies the conservation and typicality of MrSNAREs.

### 3.3. Expression Profiles of 20 MrSNAREs in Three *Monascus* Strains

The transcriptional profiles of the 20 predicted MrSNAREs in the wildtype and two mutants,  $\Delta pksCT$  and  $\Delta mrpigA$ , were firstly analyzed (Figure 5). The expression levels of *M. ruber* M7 on the 3rd day were taken as the control. Generally, compared with the 3rd day, the expression levels of most of MrSNAREs were significantly downregulated ( $p < 0.05$ ) on the 7th day. The expression patterns of different SNARE subfamilies had no obvious trend. Compared with *M. ruber* M7, for Qa-SNAREs, *Mrpep12* was significantly upregulated ( $p < 0.05$ ) in  $\Delta pksCT$  and  $\Delta mrpigA$ , while *Mrssso1*, *Mrsed5* and *Mrufe1* were significantly downregulated in the two mutants; *Mrtlg2* kept a higher expression level in  $\Delta mrpigA$  on the 3rd and 7th days. For Qb-SNAREs, only *Mroti1* was significantly upregulated ( $p < 0.05$ ) in  $\Delta pksCT$ ; the rest were all significantly downregulated; *Mrgos1* kept significantly higher expression in  $\Delta mrpigA$ , but the rest were similar to or lower than *M. ruber* M7. For Qc-SNAREs, most of them were significantly upregulated in the two mutants, except *Mrsyn8*. In addition, *Mrsec9*, the only Qbc-SNARE, was also significantly upregulated in the two mutants. Finally, regarding R-SNAREs, the expression trend of

*Mrtom* and *Mrykt6* were quite the opposite in  $\Delta pksCT$  and  $\Delta mrpigA$ , but the rest were similar. Above all, the expression of Qb-SNAREs was very different in the two mutants.

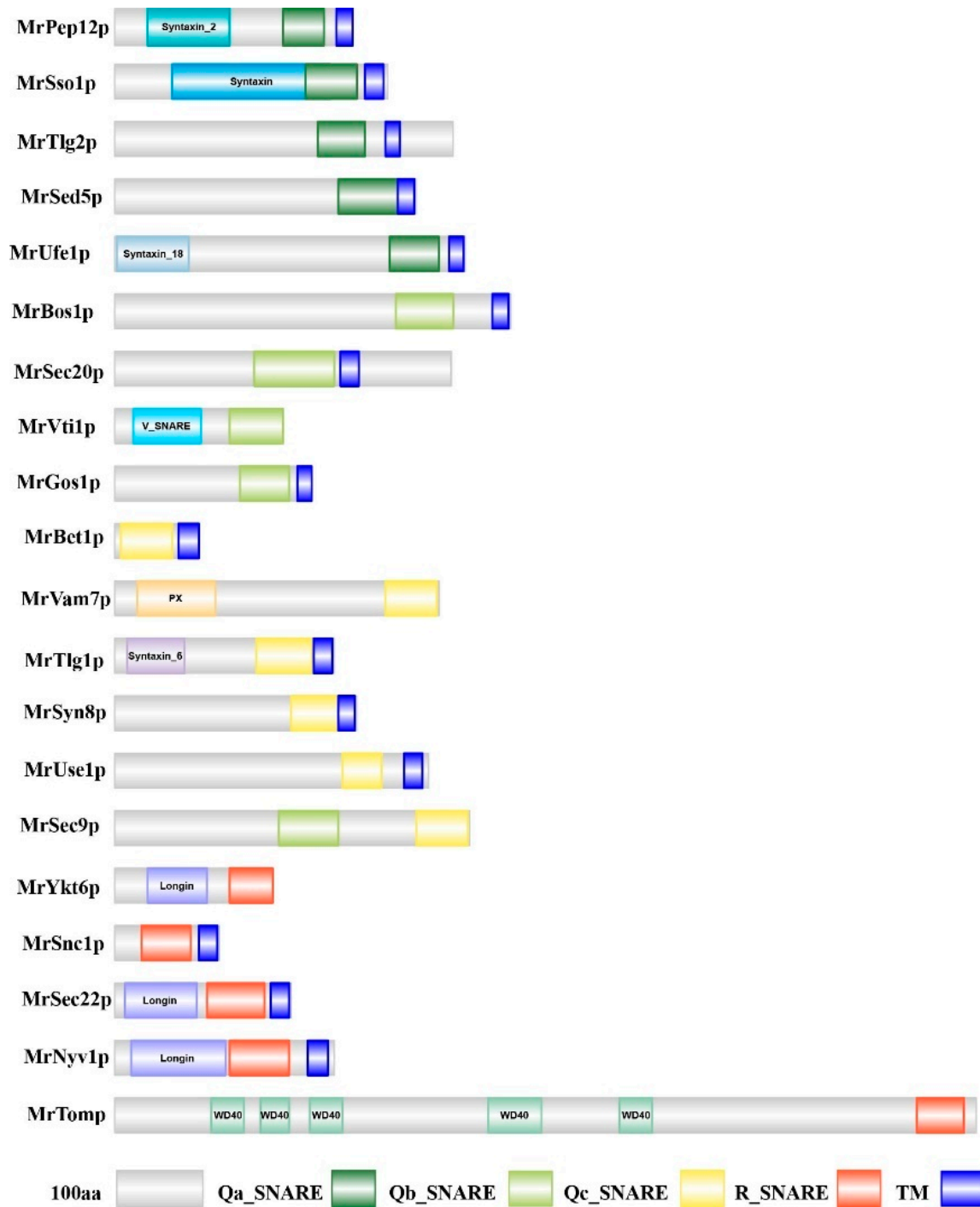


**Figure 2.** Identification of conserved domains of MrSNAREs. Dark green cylinders represent the Qa\_motif, light green cylinders represent the Qb\_motif, yellow cylinders represent the Qc\_motif, red cylinders represent the R\_motif, and blue cylinders represent the TM domain.

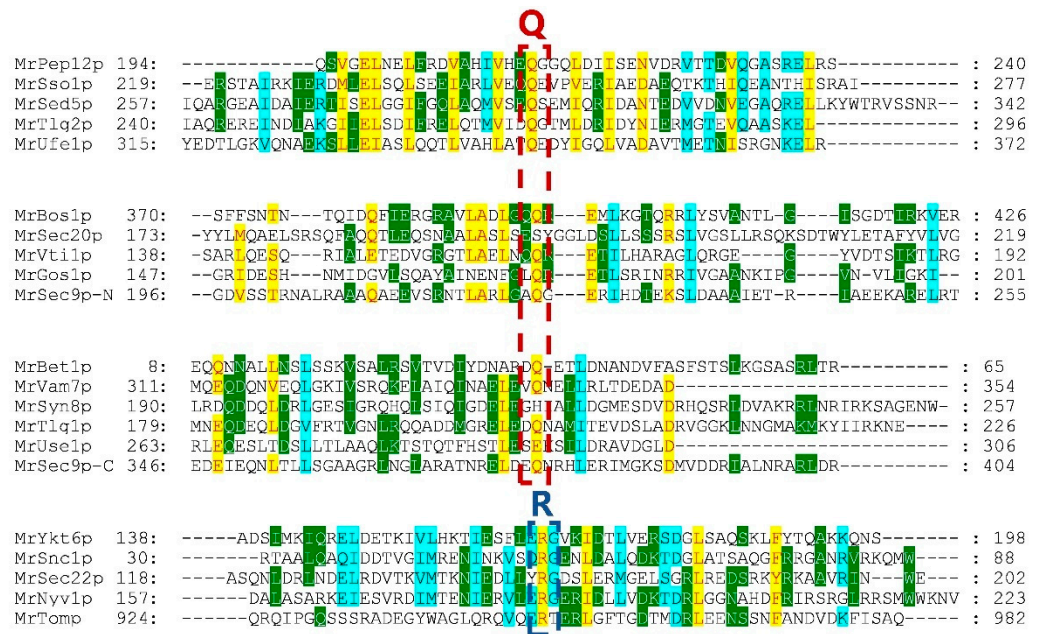


**Figure 3.** Identification of conserved residues of MrSNAREs. Red dotted boxes represent the conserved glutamine residue (Q), blue dotted boxes represent the conserved arginine residue (R).

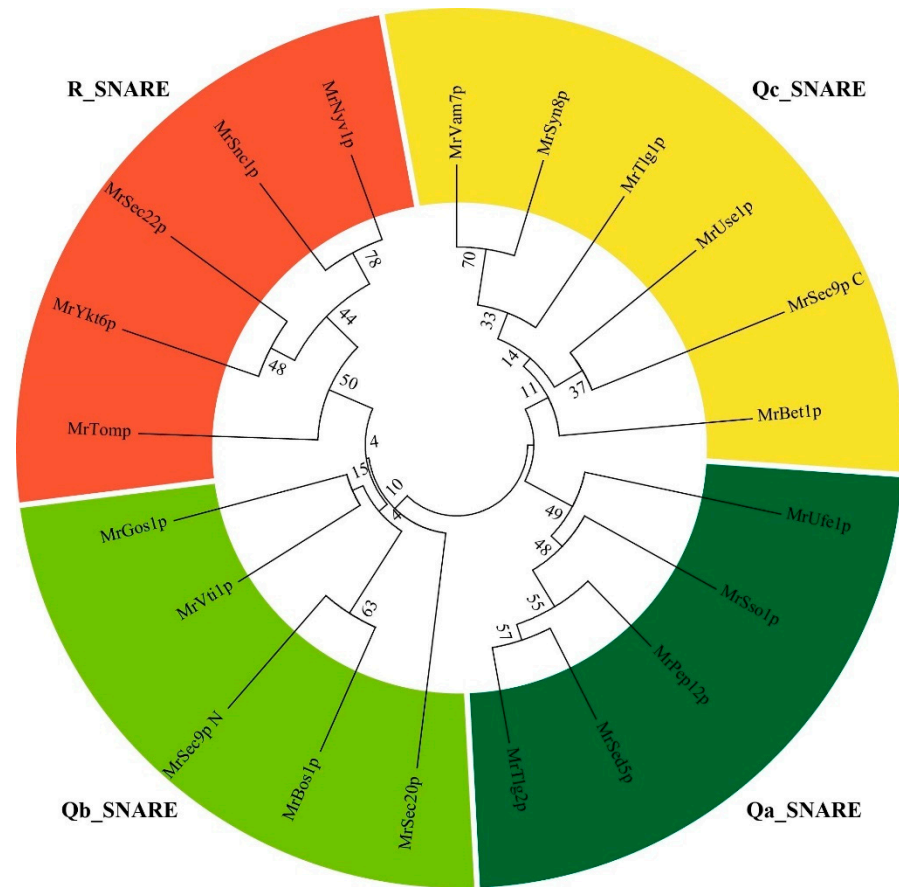


**Figure 4.** Phylogenetic analysis of 20 SNAREs identified in *M. ruber* M7. Dark green indicates Qa\_SNAREs, light green indicates Qb\_SNAREs, yellow indicates Qc\_SNAREs, and red indicates R\_SNAREs.

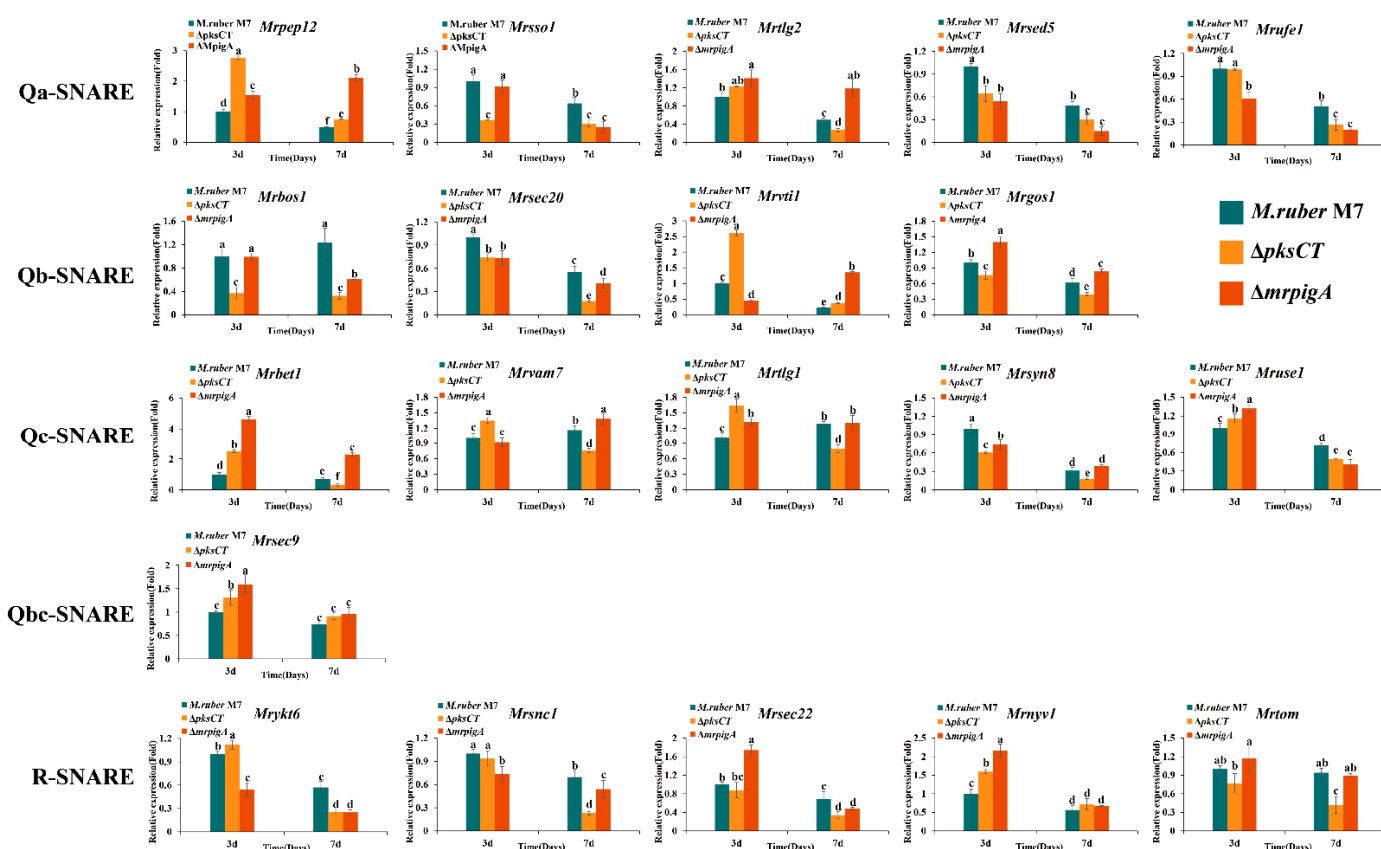


**Figure 5.** Expression profiles of the identified *MrSNAREs* in *M. ruber* M7,  $\Delta pksCT$  and  $\Delta mrpigA$ . Error bars represent means  $\pm$  SD,  $n = 3$ . Y-axis indicates the relative expression level of the genes. Different lowercase letters indicate the gene expression level is significantly different ( $p < 0.05$ ).

### 3.4. Analysis of Potential *MrSNAREs* Related to MPs and CIT Synthesis

Firstly, the phenotypic characterization and main secondary metabolite production of the wildtype and two mutants,  $\Delta pksCT$  and  $\Delta mrpigA$ , were compared. After being cultured on PDA medium for 7 days, the colony color and size of *M. ruber* M7 and  $\Delta pksCT$  were similar, but the colony of  $\Delta mrpigA$  turned from orange to white, and the colony size was obviously larger than that of *M. ruber* M7 (Figure 6a). Figure 6b shows that  $\Delta mrpigA$  had no MPs and lower CIT yield compared with *M. ruber* M7; correspondingly,  $\Delta pksCT$  had no CIT and lower MPs yield compared with *M. ruber* M7. For example, the content of CIT in  $\Delta mrpigA$  was about 45% of that in *M. ruber* M7, and the contents of YP, OP and RP in  $\Delta pksCT$  were about 83, 86 and 87% of that in *M. ruber* M7 on the 11th day. These results confirmed the remarkable differences in the secondary metabolite types of the three tested strains.

Subsequently, the expression patterns of *MrSNAREs* in *M. ruber* M7,  $\Delta mrpigA$  and  $\Delta pksCT$  were further analyzed by cluster analysis. In detail, Figure 6c shows the different expressions of *MrSNAREs* on the 3rd day among the three strains; the color (from blue to red) indicates the relative intensity change from low to high. It is obvious that there was a clear preference for the expression of *MrSNAREs* in different secondary metabolic processes. Different *MrSNAREs* gathered in two main clusters: Cluster I contained the *MrSNAREs* with higher expression levels in  $\Delta mrpigA$ , while Cluster II included the *MrSNAREs* that had higher expression levels in  $\Delta pksCT$ . This result further indicates the striking differences between *MrSNAREs* expression in the two mutants. Similarly, the expression patterns of *MrSNAREs* in the wildtype and two mutants on the 7th day also gathered in two main clusters: Cluster I contained the *MrSNAREs* that had higher expression levels in the wildtype, and Cluster II included the *MrSNAREs* that had higher expression levels in  $\Delta mrpigA$ . Further, Figure 6d was generated by the results of *M. ruber* M7-7d-1, which was

used as control. It is obviously that the difference between the two mutants was becoming smaller, so they were classified as one group when compared with the wildtype. Most of the *MrSNAREs* (12/20) gathered in the bottom part of Figure 6d were still active in  $\Delta mrpigA$ , but only four members were active in  $\Delta pksCT$ . Furthermore, the expression levels of *Mrtlg2*, *Mrbet1*, *Mrgos1* and *Mrsec22* on the 3rd and 7th days remained higher in  $\Delta mrpigA$  but lower in  $\Delta pksCT$ , which suggested a reverse response to MPs and CIT synthesis. The expression level of *Mrvtil*, *Mrvam7*, *Mrpep12* and *Mrtlg1* remained higher in  $\Delta pksCT$  but lower in  $\Delta mrpigA$  only on the 3rd day, while the expression level of these four genes was quite the opposite on the 7th day.

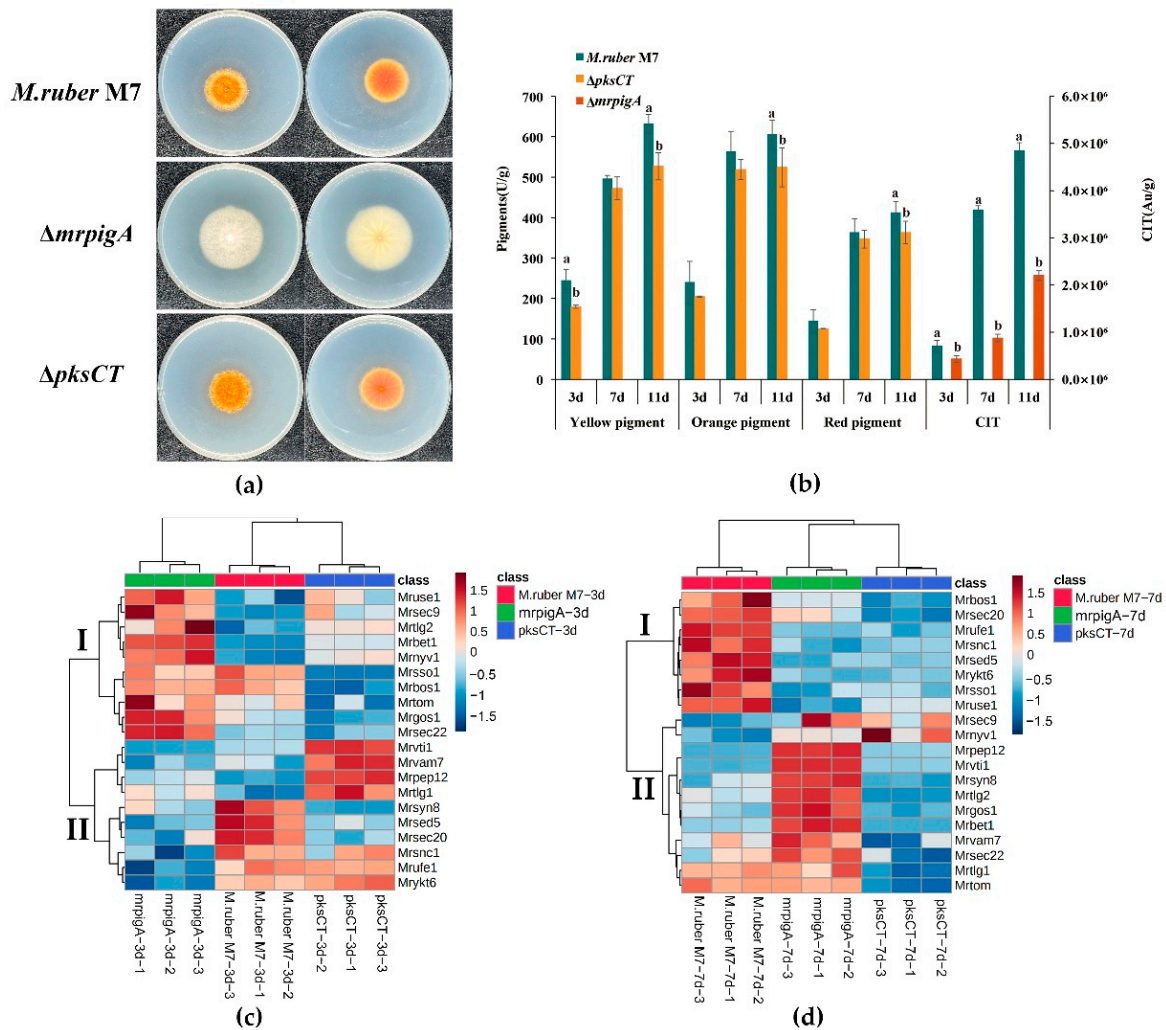


**Figure 6.** Analysis of potential SNARE genes involved in MPs and CIT synthesis. (a) Colony morphology of *M. ruber* M7,  $\Delta mrpigA$  and  $\Delta pksCT$  on PDA plate after cultivating at 28 °C for 7 days. (b) MPs and CIT produced by *M. ruber* M7,  $\Delta mrpigA$  and  $\Delta pksCT$ . Different lowercase letters indicate the gene expression level is significantly different ( $p < 0.05$ ). (c) Heatmap based on relative expression levels of *MrSNAREs* on the 3rd day; the expression level of *M. ruber* M7-3d-1 is the control. (d) Heatmap based on the relative expression levels of *MrSNAREs* on the 7th day; the expression level of *M. ruber* M7-7d-1 is the control.

#### 4. Discussion

SNAREs play a central role in achieving precise material transport between membrane vesicles and have been shown to have important functions in regulating of secondary metabolites. Usually, more than 20 *SNARE* genes can be identified in most filamentous fungi genomes, and they perform conserved functions during specific vesicle transport

pathways [38]. Further, duplicate members of SNARE genes have been reported in *S. cerevisiae*, such as *Sso2* (*Sso1* duplicate gene), *Snc2* (*Snc1* double gene), *Vam3* (*Pep12* duplicate gene) and *Spo20* (*Sec9* duplicate gene) [39,40]. In this study, 20 SNARE genes were identified in the *M. ruber* M7 genome; the most remarkable difference was the absence of *Sft1* homologs. A previous study reported that deletion of *Sft1* in *S. cerevisiae* can be compensated for by *Bet1* overexpression, indicating that *Bet1* in *M. ruber* M7 could perform the function of *Sft1* [41]. Therefore, the 20 SNAREs seemed to fulfill the requirements of vesicular trafficking of *M. ruber* M7.

In the current study, *Mrtom*, a large gene organized in seven exons that span 2997 bp, was identified in the *M. ruber* M7 genome. Although its gene structure and amino acid structure were different from those of other *MrSNAREs*, its C-terminal still contained the SNARE motif, suggesting that it could act as SNAREs in *M. ruber* M7. Further, the glutamine residues (Q-site) of *Sec20*, *Syn8* and *Use1* were replaced by serine (S), histidine (H) and glutamic (E), respectively. Similar divergences were noted previously in most fungi, as well as in plants and animals [42,43]. These results suggested that the function of these special SNARE genes may be inconsistent across organisms.

Previous studies have illustrated that MPs and CIT share the same initial synthetic pathway but have independent biosynthetic gene clusters [44,45]; this is not enough to reveal the puzzling interaction between the synthesis of MPs and CIT. Recently, the study of compartmentalized biosynthesis of fungal natural products has been a hot topic, which depends on highly ordered subcellular compartmentalization and trafficking of biosynthetic enzymes and their intermediates through vesicles [46]. It is well-known that SNAREs are the core component mediating vesicle trafficking and have a significant role in the secondary metabolism in filamentous fungi. Our study indicates that the expression profiles of SNAREs in  $\Delta pksCT$  and  $\Delta mrpigA$  are significantly different, suggesting that *MrSNAREs* may be involved in the specific regulation of MPs and CIT biosynthesis. Therefore, further investigation of the functions of *MrSNAREs* could help to reveal whether SNARE could provide reverse regulation of the production of MPs and citrinin and could provide a new strategy for the construction of engineered *Monascus* strains with high yield of MPs and low or no yield of CIT.

Additionally, the heatmap of expression profiles of all identified *MrSNAREs* was performed by MetaboAnalyst, which is a widely accepted tool to deal with metabolomics data [47]. In our study, we extended its application to the cluster analysis of the results of relative expression levels of *MrSNAREs*; then, we arranged the clustering results in Microsoft Office Excel 2019 and applied a graded color scale from the conditional formatting gallery. The result shows good classification, and the most-differentially expressed genes can be easily found (Table S2). Thus, MetaboAnalyst is also helpful for statistical analysis of qRT-PCR results.

## 5. Conclusions

The comprehensive characterization of the SNARE family by genome-wide analysis in *Monascus* spp. is performed for the first time in this study. Here, we identify and characterize 20 SNARE genes in *Monascus ruber* M7 (*MrSNAREs*), which we could divide into four groups based on conserved motifs and phylogenetic relationships. The expression profiles of these *MrSNAREs* are compared in *M. ruber* M7,  $\Delta pksCT$  and  $\Delta mrpigA$ ; three strains have significant differences in their kinds of secondary metabolites. The expression patterns of 20 *MrSNAREs* show obvious distinct distributions in these three strains. *Mrtlg2*, *Mrbet1*, *Mrgos1* and *Mrsec22* could be considered potential candidate genes involved in the regulation of MPs and CIT synthesis for further functional characterization. Taken together, these results promote the understanding of the SNARE family and provide new insights into their function in secondary metabolism of filamentous fungi.

**Supplementary Materials:** The following supporting information can be downloaded at: <https://www.mdpi.com/article/10.3390/fermentation8120750/s1>, Table S1: RT-qPCR primers used in this study; Table S2: Expression profiles of all identified *MrSNAREs* in *M. ruber* M7,  $\Delta mrpigA$  and  $\Delta pksCT$ .

**Author Contributions:** Conceptualization, J.L.; methodology, J.L. and C.M.; investigation, C.M.; writing—original draft preparation, J.L. and C.M.; writing—review and editing, J.L. and Y.Z.; visualization, J.L. and C.M.; supervision, Y.Z. and F.C.; funding acquisition, Y.Z. and F.C. All authors have read and agreed to the published version of the manuscript.

**Funding:** This research was funded by the Major Programs (No. 31730068 and No. 31330059 to FC) and the Young Scientist Program (No. 31701583 to JL) of the National Natural Science Foundation of China.

**Institutional Review Board Statement:** Not applicable.

**Informed Consent Statement:** Not applicable.

**Data Availability Statement:** Not applicable.

**Conflicts of Interest:** The authors declare no conflict of interest.

## References

- Behnia, R.; Munro, S. Organelle identity and the signposts for membrane traffic. *Nature* **2005**, *438*, 597–604. [[CrossRef](#)] [[PubMed](#)]
- Spang, A. The life cycle of a transport vesicle. *Cell Mol. Life Sci.* **2008**, *65*, 2781–2789. [[CrossRef](#)] [[PubMed](#)]
- Higuchi, Y. Membrane traffic related to endosome dynamics and protein secretion in filamentous fungi. *Biosci. Biotechnol. Biochem.* **2021**, *85*, 1038–1045. [[CrossRef](#)] [[PubMed](#)]
- Gillingham, A.K.; Munro, S. Transport carrier tethering—How vesicles are captured by organelles. *Curr. Opin. Cell Biol.* **2019**, *59*, 140–146. [[CrossRef](#)]
- Margiotta, A. Membrane fusion and snares: Interaction with ras proteins. *Int. J. Mol. Sci.* **2022**, *23*, 8067. [[CrossRef](#)]
- Koike, S.; Jahn, R. SNARE proteins: Zip codes in vesicle targeting? *Biochem. J.* **2022**, *479*, 273–288. [[CrossRef](#)]
- Heo, P.; Coleman, J.; Fleury, J.B.; Rothman, J.E.; Pincet, F. Nascent fusion pore opening monitored at single-SNAREpin resolution. *Proc. Natl. Acad. Sci. USA* **2021**, *118*, e2024922118. [[CrossRef](#)]
- Hong, W.; Lev, S. Tethering the assembly of SNARE complexes. *Trends Cell Biol.* **2014**, *24*, 35–43. [[CrossRef](#)]
- Van den Bogaart, G.; Lang, T.; Jahn, R. *Chapter Six—Microdomains of Snare Proteins in the Plasma Membrane*, in *Current Topics in Membranes*; Bennett, V., Ed.; Academic Press: Cambridge, MA, USA, 2013; pp. 193–230.
- Fasshauer, D.; Sutton, R.B.; Brunger, A.T.; Jahn, R. Conserved structural features of the synaptic fusion complex: SNARE proteins reclassified as Q- and R-SNAREs. *Proc. Natl. Acad. Sci. USA* **1998**, *95*, 15781–15786. [[CrossRef](#)]
- Jahn, R.; Scheller, R.H. SNAREs—Engines for membrane fusion. *Nat. Rev. Mol. Cell Biol.* **2006**, *7*, 631–643. [[CrossRef](#)]
- Han, J.; Pluhackova, K.; Böckmann, R.A. The multifaceted role of snare proteins in membrane fusion. *Front. Physiol.* **2017**, *8*, 5. [[CrossRef](#)] [[PubMed](#)]
- Hong, W. SNAREs and traffic. *BBA-Mol. Cell Res.* **2005**, *1744*, 120–144. [[CrossRef](#)] [[PubMed](#)]
- Chen, Y.A.; Scheller, R.H. SNARE-mediated membrane fusion. *Nat. Rev. Mol. Cell Biol.* **2001**, *2*, 98–106. [[CrossRef](#)] [[PubMed](#)]
- Söllner, T.; Whiteheart, S.W.; Brunner, M.; Erdjument-Bromage, H.; Geromanos, S.; Tempst, P.; Rothman, J.E. SNAP receptors implicated in vesicle targeting and fusion. *Nature* **1993**, *362*, 318–324. [[CrossRef](#)] [[PubMed](#)]
- Burri, L.; Lithgow, T. A complete set of SNAREs in yeast. *Traffic* **2004**, *5*, 45–52. [[CrossRef](#)]
- Pratelli, R.; Sutter, J.U.; Blatt, M.R. A new catch in the SNARE. *Trends Plant Sci.* **2004**, *9*, 187–195. [[CrossRef](#)]
- Adnan, M.; Islam, W.; Noman, A.; Hussain, A.; Anwar, M.; Khan, M.U.; Akram, W.; Ashraf, M.F.; Raza, M.F. Q-SNARE protein FgSyn8 plays important role in growth, DON production and pathogenicity of *Fusarium graminearum*. *Microb. Pathog.* **2020**, *140*, 103948. [[CrossRef](#)]
- Li, S.; Zhang, S.; Li, B.; Li, H. The SNARE protein *cfvam7* is required for growth, endoplasmic reticulum stress response, and pathogenicity of *Colletotrichum fructicola*. *Front. Microbiol.* **2021**, *12*, 736066. [[CrossRef](#)]
- Li, B.; Gao, Y.; Mao, H.Y.; Borkovich, K.A.; Ouyang, S.Q. The SNARE protein *FolVam7* mediates intracellular trafficking to regulate conidiogenesis and pathogenicity in *Fusarium oxysporum* f. sp. *lycopersici*. *Environ. Microbiol.* **2019**, *21*, 2696–2706. [[CrossRef](#)]
- Su, Z.Z.; Dai, M.D.; Zhu, J.N.; Liu, X.H.; Li, L.; Zhu, X.M.; Wang, J.Y.; Yuan, Z.L.; Lin, F.C. Dark septate endophyte *Falciphora oryzae*-assisted alleviation of cadmium in rice. *J. Hazard. Mater.* **2021**, *419*, 126435. [[CrossRef](#)]
- Adnan, M.; Islam, W.; Zhang, J.; Zheng, W.; Lu, G.D. Diverse role of SNARE protein *Sec22* in vesicle trafficking, membrane fusion, and autophagy. *Cells* **2019**, *8*, 337. [[CrossRef](#)] [[PubMed](#)]
- O'Mara, S.P.; Broz, K.; Boenisch, M.; Zhong, Z.; Dong, Y.; Kistler, H.C. The *Fusarium graminearum* t-SNARE *Sso2* is involved in growth, defense, and don accumulation and virulence. *Mol. Plant Microbe Interact.* **2020**, *33*, 888–901. [[CrossRef](#)] [[PubMed](#)]

24. Qi, Z.; Liu, M.; Dong, Y.; Zhu, Q.; Li, L.; Li, B.; Yang, J.; Li, Y.; Ru, Y.; Zhang, H.; et al. The syntaxin protein (MoSyn8) mediates intracellular trafficking to regulate conidiogenesis and pathogenicity of rice blast fungus. *New Phytol.* **2016**, *209*, 1655–1667. [[CrossRef](#)] [[PubMed](#)]
25. Chen, W.; He, Y.; Zhou, Y.; Shao, Y.; Feng, Y.; Li, M.; Chen, F. Edible filamentous fungi from the species *Monascus*: Early traditional fermentations, modern molecular biology, and future genomics. *Compr. Rev. Food Sci. Food Saf.* **2015**, *14*, 555–567. [[CrossRef](#)]
26. Chen, W.; Feng, Y.; Molnár, I.; Chen, F. Nature and nurture: Confluence of pathway determinism with metabolic and chemical serendipity diversifies *Monascus* azaphilone pigments. *Nat. Prod. Rep.* **2019**, *36*, 561–572. [[CrossRef](#)]
27. Zhang, C.; Chen, M.; Zang, Y.; Wang, H.; Wei, X.; Zhu, Q.; Yang, X.; Sun, B.; Wang, C. Effect of arginine supplementation on Monacolin K yield of *Monascus purpureus*. *J. Food Compos. Anal.* **2022**, *106*, 104252. [[CrossRef](#)]
28. Hou, Y.; Liu, J.; Shao, Y.; Peng, X.; Zhang, D.; Hu, L.; Chen, F.; Zhou, Y. Evaluation of the underestimation of citrinin content in Hongqu using hydrolysis treatments and UPLC-FLD. *Food Control* **2021**, *130*, 108245. [[CrossRef](#)]
29. Righetti, L.; Dall’Asta, C.; Bruni, R. Risk assessment of ryr food supplements: Perception vs. reality. *Front. Nutr.* **2021**, *8*, 792529. [[CrossRef](#)]
30. Liu, W.; An, C.; Shu, X.; Meng, X.; Yao, Y.; Zhang, J.; Chen, F.; Xiang, H.; Yang, S.; Gao, X.; et al. A dual-plasmid crispr/cas system for mycotoxin elimination in polykaryotic industrial fungi. *ACS Synth. Biol.* **2020**, *9*, 2087–2095. [[CrossRef](#)]
31. Ning, Z.Q.; Cui, H.; Xu, Y.; Huang, Z.B.; Tu, Z.; Li, Y.P. Deleting the citrinin biosynthesis-related gene, *ctnE*, to greatly reduce citrinin production in *Monascus aurantiacus* Li AS3.4384. *Int. J. Food Microbiol.* **2017**, *241*, 325–330. [[CrossRef](#)]
32. Xie, N. Identification and Exploration of Pigment Gene Cluster and Metabolic Pathway in *Monascus ruber* M-7. Ph.D. Thesis, Huazhong Agricultural University, Wuhan, China, 2013; pp. 52–57.
33. Chen, W.; Chen, R.; Liu, Q.; He, Y.; He, K.; Ding, X.; Kang, L.; Guo, X.; Xie, N.; Zhou, Y.; et al. Orange, red, yellow: Biosynthesis of azaphilone pigments in *Monascus* fungi. *Chem. Sci.* **2017**, *8*, 4917–4925. [[CrossRef](#)] [[PubMed](#)]
34. He, Y. Construction of a High-Efficiency Gene Knockout System of *Monascus ruber* M7 and Analysis of the Biosynthetic Pathway of Citrinin. Ph.D. Thesis, Huazhong Agricultural University, Wuhan, China, 2015; pp. 113–118.
35. He, Y.; Cox, R.J. The molecular steps of citrinin biosynthesis in fungi. *Chem. Sci.* **2016**, *7*, 2119–2127. [[CrossRef](#)] [[PubMed](#)]
36. Li, W.; Li, Y.; Yu, W.; Li, A.; Wang, Y. Study on production of yellow pigment from potato fermented by *Monascus*. *Food Biosci.* **2022**, *50*, 102088. [[CrossRef](#)]
37. Huang, Z.; Hu, T.; Liu, H.; Xie, H.; Tian, X.; Wu, Z. Biosynthesis and polyketide oxidation of *Monascus* red pigments in an integrated fermentation system with microparticles and surfactants. *Food Chem.* **2022**, *394*, 133545. [[CrossRef](#)] [[PubMed](#)]
38. Li, X.; Xiong, D.; Tian, C. Genome-wide identification, phylogeny and transcriptional profiling of SNARE genes in *Cytospora chrysosperma*. *J. Phytopathol.* **2021**, *169*, 471–485. [[CrossRef](#)]
39. Khurana, G.K.; Vishwakarma, P.; Puri, N.; Lynn, A.M. Phylogenetic analysis of the vesicular fusion SNARE machinery revealing its functional divergence across Eukaryotes. *Bioinformatics* **2018**, *14*, 361–368. [[CrossRef](#)]
40. Grissom, J.H.; Segarra, V.A.; Chi, R.J. New perspectives on snare function in the yeast minimal endomembrane system. *Genes* **2020**, *11*, 899. [[CrossRef](#)]
41. Tsui, M.; Banfield, D. Yeast Golgi SNARE interactions are promiscuous. *J. Cell Sci.* **2000**, *113*, 145–152. [[CrossRef](#)]
42. Dilcher, M.; Veith, B.; Chidambaram, S.; Hartmann, E.; Schmitt, H.D.; von Mollard, G.F. Use1p is a yeast SNARE protein required for retrograde traffic to the ER. *EMBO J.* **2003**, *22*, 3664–3674. [[CrossRef](#)]
43. Kádková, A.; Radecke, J.; Sørensen, J.B. The SNAP-25 protein family. *Neuroscience* **2019**, *420*, 50–71. [[CrossRef](#)]
44. Li, L.; Xu, N.; Chen, F. Inactivation of *mrpigH* gene in *Monascus ruber* M7 results in increased *Monascus* pigments and decreased citrinin with *mrpyrG* selection marker. *J. Fungi* **2021**, *7*, 1094. [[CrossRef](#)] [[PubMed](#)]
45. Wang, J.; Huang, Y.; Shao, Y. From traditional application to genetic mechanism: Opinions on *Monascus* research in the new milestone. *Front. Microbiol.* **2021**, *12*, 659907. [[CrossRef](#)] [[PubMed](#)]
46. Du, L.; Li, S. Compartmentalized biosynthesis of fungal natural products. *Curr. Opin. Biotechnol.* **2021**, *69*, 128–135. [[CrossRef](#)] [[PubMed](#)]
47. Pang, Z.; Zhou, G.; Ewald, J.; Chang, L.; Hacariz, O.; Basu, N.; Xia, J. Using MetaboAnalyst 5.0 for LC–HRMS spectra processing, multi-omics integration and covariate adjustment of global metabolomics data. *Nat. Protoc.* **2022**, *17*, 1735–1761. [[CrossRef](#)]